



Acetylated Cellulose/Polyethylene Glycol Composite Membranes for Removal of Polycyclic Aromatic Hydrocarbons from Marine Sediments

Muhammad Syahrir¹, Muhammad Danial Sanusi¹, Muhammad Nur Alam^{1*}, Rizal Irfandi¹, Dian Permana², Subakir Salnus¹

¹ Department of Chemistry, Universitas Negeri Makassar, Makassar 90244, Indonesia

² Science Education Study Program, Universitas Sembilanbelas November Kolaka, Kolaka 93514, Indonesia

Corresponding Author Email: m.nur.alam@unm.ac.id

Copyright: ©2025 The authors. This article is published by IIETA and is licensed under the CC BY 4.0 license (<http://creativecommons.org/licenses/by/4.0/>).

<https://doi.org/10.18280/ij dne.200301>

ABSTRACT

Received: 12 December 2024

Revised: 18 January 2025

Accepted: 26 January 2025

Available online: 31 March 2025

Keywords:

cellulose acetate, membrane, phase inversion, polycyclic aromatic hydrocarbons, pollutant

Cellulose acetate (CA)/polyethylene glycol (PEG) composite membranes are promising advanced materials for the removal of polycyclic aromatic hydrocarbons (PAHs) from wastewater. Therefore, this study aimed at synthesizing CA/PEG composite membranes using the phase inversion method with CA/PEG composition ratios (w/w) of 12:6, 13:5, 14:4, and 15:3. The synthesis process began with the acetylation of cellulose to produce CA, and the obtained products were characterized using ATR-FTIR, SEM, and TGA. The water contact angle (WCA) and swelling index (SI) were evaluated to determine the hydrophobicity. The results showed that the CA/PEG (15:3) membrane had the highest water contact angle and the lowest swelling index, indicating its superior hydrophobic characteristics. FTIR analysis confirmed the successful synthesis by identifying characteristic peaks of CA and PEG, particularly at 3300 cm⁻¹ (associated with -OH groups), 1049 cm⁻¹, and 617 cm⁻¹ (corresponding to C-O and -OH torsional vibrations). In addition, SEM images revealed a less porous surface with non-uniform pore sizes across the products. TGA analysis indicated that the CA/PEG (14:4) membrane had the best thermal stability, evidenced by the lowest weight loss percentage of 70.64%. The evaluation of water flux indicated the CA/PEG (12:6) membrane achieved the highest flux value of 54.081 L/m²·h. Conversely, the CA/PEG (14:4) membrane exhibited superior anti-fouling performance, with the highest FRR value of 84.62, demonstrating its consistency. Furthermore, the CA/PEG (14:4) membrane testing on real samples of marine sediment extract confirmed the maximum rejection rate of pyrene compound of 87.67%. These results demonstrate the high effectiveness and efficiency of cellulose acetate-based membranes in removing PAHs from wastewater. Moreover, this membrane is renewable and environmentally friendly.

1. INTRODUCTION

Polycyclic aromatic hydrocarbons (PAHs) are persistent organic pollutants that are resistant to degradation and consist of two or more fused benzene rings [1, 2]. PAHs are frequently detected in marine environments, originating from multiple sources such as incomplete combustion or pyrolysis of carbon- and hydrogen-rich materials, including coal, petroleum, wood, and their derivatives. Numerous studies have indicated that pollution from these substances enters marine ecosystems through various industrial wastewater discharges, such as effluents from the oil and gas sector, pharmaceutical production, and coking facilities, along with leachates from municipal landfills [3]. PAHs have significant impacts on human health and the environment [4, 5]. Therefore, it is imperative to reduce their levels in wastewater from WWTP effluent before it is discharged into the ocean. Various PAHs reduction methods have been investigated, including adsorption, chemical degradation, biodegradation, and membrane filtration [6]. However, completely removing these

materials using traditional methods, such as chemical, biological, and physical treatment, is often difficult and can produce toxic by-products [7]. In line with these findings, filtration with membranes, particularly nanofiltration (NF) technology, has attracted attention due to its unique separation capabilities and low energy consumption. Polyethersulfone (PES) membranes are one of the most widely used due to their high oxidative stability, thermal stability, and mechanical properties [8]. However, the poor hydrophilic nature is responsible for their susceptibility to fouling by organic contaminants, leading to high energy requirements and short lifetime. From an economic aspect, PES-based membranes are fairly expensive because the raw materials are sourced from synthetic chemicals [5]. This suggests that the membranes developed in this study are expected to exhibit superior performance in PAH separation and be environmentally friendly, in alignment with the Sustainable Development Goals (SDGs).

Cellulose acetate (CA)-based membranes are one of the materials being explored in the current study due to their wide

application for seawater desalination, separation of organic and inorganic materials, microorganisms, BSA, and others [9]. However, studies on PAHs separation using biopolymer-based membranes have not been conducted. Cellulose acetate is synthesized through the cellulose acetylation process, which can be obtained from various types of wood-based lignocellulosic materials or fibers that are abundant, such as oil palm, Nipah fronds, seaweed, and others. Cellulose acetate offers several advantages as a membrane material, including low processing costs, high selectivity in the absorption process, solubility in various solvents, excellent hydrophilicity, and its origin from renewable natural resources [9]. Various efforts to improve membrane performance, particularly in overcoming fouling issues in water purification, are continuously pursued. For example, Chen et al. [10] modified PES-based membranes with ZrO₂ nanoparticle coating material with the aim of increasing the value of water flux and PAHs rejection. The results showed that coating with ZrO₂ increased the PAHs rejection value 4 times higher to reach 90%.

Abedini et al. [11] also reported an increase in hydrophilicity and humic acid rejection rate of 97% in the modification of PES membranes by coating with nanozirconia particles, where the optimum coating was achieved at 5% nanoparticle incorporation. Previous studies have shown that polyethylene glycol (PEG) is one of the polymeric materials with high hydrophilicity properties and can play a role in increasing water flux and antifouling properties. Fathy et al. [12] synthesized CA/polystyrene membranes that were grafted with PEG to increase the rejection value of kaolin to 99%. Bhattacharjee and Datta [13] identified the effect of PEG molecular weight on CA membranes for dialysis applications and found that PEG 200 could improve the cleaning performance and permeability to urea. In addition, increasing the amount of PEG above 10% did not improve the membranes' performance. In this study, CA membranes were modified through the addition of PEG at various composition ratios of CA and PEG to form composite membranes. Although cellulose acetate-PEG composite membranes have been developed, their application to the filtration of PAHs pollutant compounds has not been explored, especially in antifouling studies. Therefore, this study aims to improve PAH removal performance by optimizing the composition of the CA/PEG composite membrane, as well as to evaluate its antifouling properties and thermal stability.

2. MATERIAL AND METHODS

2.1 Materials

The materials used in this study were cellulose from sigma-Aldrich, glacial acetic acid (Merck brand), anhydride acetate (Merck brand), Sulphuric Acid (H₂SO₄) purify: 95-97% Merck brand), NaOH powder, polyethylene glycol (PEG 600, Merck brand), dimethylformamide (DMF, Merck brand), deionized water, aqua dest, and PAHs solution (pyrene, benzo(a)anthracene, perylene).

2.2 Acetylation of cellulose

A total of 50 g of cellulose was dissolved in 500 mL of glacial acetic acid in a reaction flask and stirred for 3 hours. Subsequently, 30 mL of acetic anhydride and 6 drops of H₂SO₄ were added, and the reaction mixture was stirred at 70°C for

2.5 hours. The selection of a temperature of 70°C and a reaction time of 2.5 h was based on the optimization results showing that these conditions provided maximum efficiency in replacing cellulose hydroxyl groups with acetyl groups without causing degradation of the cellulose polymer structure, as reported in a previous study [14]. Then, 5 mL of deionised water and 10 mL of glacial acetic acid were added to stop the reaction, followed by stirring for 30 minutes. Then, 5 g of sodium acetate was incorporated to neutralize excess acid, stirred for 5 minutes, thoroughly washed with distilled water, soaked in methanol for 10 minutes to remove residual reagents and acetic acid by-products, and dried in an oven at 45°C for 18 hours. The CA powder was analyzed for acetyl content and functional group identification with an FTIR spectrometer [15].

2.3 Analysis of acetyl content

1 g of CA and 40 mL of 70% ethanol were placed inside the Erlenmeyer, and the mixture was heated to 55°C in a bath for 30 minutes. A total of 40 mL of 0.5 N NaOH was added to the mixture and heated in a water bath for 15 minutes at 55°C. Then, it was covered with foil and allowed to sit for a full day. After adding 2 drops of pp indicator, the mixture was covered again and let to stand for 24 hours. At that point, 0.5 N HCl was added, and the volume needed for the titration was noted after adding the pp indicator titrate using 0.5 N NaOH, which ascertained the acetyl groups (AG) based on Eq. (1) [9].

$$AG (\%) = \frac{(V_{bi} - V_{bt})\mu_b - V_a|43}{M_{ca}} \times 100\% \quad (1)$$

where, % AG was a percentage of acetylated groups, and V_{bi} was the volume of NaOH added to the system and lost in the titration. In addition, μ_b was the NaOH concentration, V_a was the volume of HCl added to the system, 43 was the molecular mass of the acetyl groups, and M_{ca} was the weight of the CA sample.

2.4 Fabrication of cellulose acetate/PEG membrane

Cellulose acetate/PEG membranes were fabricated through the phase inversion method. The casting solution was prepared by dissolving cellulose acetate and PEG in various weight ratios (12:6, 13:5, 14:4, 15:3) in 10 mL of dimethylformamide (DMF). This mixture was stirred continuously at 60°C for 6 hours to ensure complete homogenization. Following this, the solution was sonicated using an ultrasonic cleaner to remove any entrapped air bubbles. After resting overnight, the solution was cast onto a smooth glass plate, held at room temperature for 30 seconds, and then immersed in a water coagulation bath. The resulting membrane was stored in deionized water until further analysis [16].

2.5 Physicochemical properties of the membrane

The physicochemical properties of the membrane identified were the swelling index and water-contact angle (WHC). This was identified by following the procedure [17], in which a cellulose sample (2×2 cm²) was dispersed in deionized water. The swelling index was calculated using Eq. (2).

$$SI (\%) = \frac{M_1 - M_0}{M_0} \times 100\% \quad (2)$$

where, SI was denoted by the swelling index, and M₁ and M₀

denoted the weights of the swollen and the dry sample. The water contact angle (WCA) was measured using a previously reported method [18].

The dried flat membrane samples were cut into pieces measuring 10 mm × 5 mm and positioned on a glass slide. Deionized water droplets were carefully applied to the membrane surface, and images of these droplets were captured. The contact angle was then measured using ImageJ software. To ensure precision, the water contact angle (WCA) test was conducted three times for each membrane, and the average value was calculated.

2.6 FTIR analysis

Membrane samples were characterized for functional groups using ATR-FTIR in the solid state. The infrared spectra were recorded in the 4000 to 650 cm⁻¹ range with an ATR-FTIR spectrophotometer (Bruker IFS 113v) [19].

2.7 Morphological properties

The morphology of membrane samples was identified using SEM (JEOL) at accelerating voltage 15.0 kV and magnification from 50 to 2000x for the membrane surface and 100 to 3000x for the cross-section (thickness). Before SEM analysis, the specimens were dried in a vacuum oven at 40°C for 2 days to remove residual solvent or water from the membrane and prevent structural deformation. The CA/PEG membranes were cryogenically fractured in liquid nitrogen to prepare cross-sectional samples. Subsequently, the specimens were mounted on aluminum stubs with double-sided conductive tape and sputter-coated (Techincs EMS, Inc, VA) with a thin layer of gold for 30 minutes. The ratio of sample and gold palladium was 60:40 [16].

2.8 TGA analysis

Thermogravimetric analysis (TGA) was performed to assess the decomposition temperature and thermal stability using a Linseis STA PT-1000 instrument. The decomposition behavior was examined over a temperature range of 28°C to 700°C at a heating rate of 10°C/min under an air atmosphere. Additionally, differential scanning calorimetry (DSC) thermograms were obtained by heating the sample from room temperature to 700°C.

2.9 Application in PAHs removals

2.9.1 Water flux

Water flux was determined by following the procedure [20]. A membrane with a diameter of 5 cm was placed on the membrane holding the vacuum filtration device and then clamped tightly. A total of 100 mL of PAHs (pyrene, benzo(a)anthracene, perylene) in an aqueous solution was put into the feed container. The solution was flowed through the membrane with a pump pressure of 1 bar for 1/8 hour. The solution that passed through this was collected in the permeate container, and the flux value was calculated using Eq. (3):

$$J = \frac{V}{A t} \quad (3)$$

where, J was water flux (L/m²h), A was membrane surface area (m²), V was permeate volume (L), and t was time (hours).

2.9.2 Antifouling test

The antifouling properties were determined based on the Flux Recovery Ratio (FRR) value calculated using Eq. (4).

$$FRR (\%) = \frac{J_{wc}}{J_{wo}} \times 100 \% \quad (4)$$

where, FRR was the Flux Recovery Ratio, J_{wo} was the initial flux, and J_{wc} was the flux after the membrane washing process [19].

2.9.3 Rejection of PAHs

The rejection of CA/PEG membranes to PAHs pollutants was determined using GC-MS. Firstly, 3 samples of marine sediment extracts (MSE) obtained from the waters of the Makassar strait at 3 regions denoted TG₁, TG₂, and TG₃ were analyzed using GC-MS to determine initial PAHs concentration (C_f). This was carried out using 7 standard PAHs compounds (naphthalene, acenaphthene, fluoranthene, pyrene, benzo(a)anthracene, phenanthrene, and perylene) [21, 22]. Secondly, 4 sample MSEs were filtered using a vacuum filtration device equipped with CA/PEG membranes. This process was carried out for 30 minutes at room temperature with a pressure of 1 bar. The permeate solution was analyzed using GC-MS to determine the detected PAHs concentration (C_p). Then, the membrane rejection of PAHs compounds was calculated using the Eq. (5).

$$R (\%) = \frac{C_f - C_p}{C_f} \times 100\% \quad (5)$$

where, R was membrane rejection to PAHs, C_f was PAHs concentration before filtration, and C_p was detected PAHs concentration after filtration with membrane.

3. RESULT AND DISCUSSION

3.1 Acetylation of cellulose

The result of cellulose acetylation at 70°C had produced a white-colored CA powder (see Figure 1) of 24.83 g with a yield of 49.66%, respectively. These results showed that the acetylation process went well. The CA produced had a degree of acetylation of 43.03%.



Figure 1. Cellulose acetate powder

The formation of CA from the cellulose acetylation process was confirmed by the results of the FTIR analysis between cellulose and cellulose acetate in Figure 2.

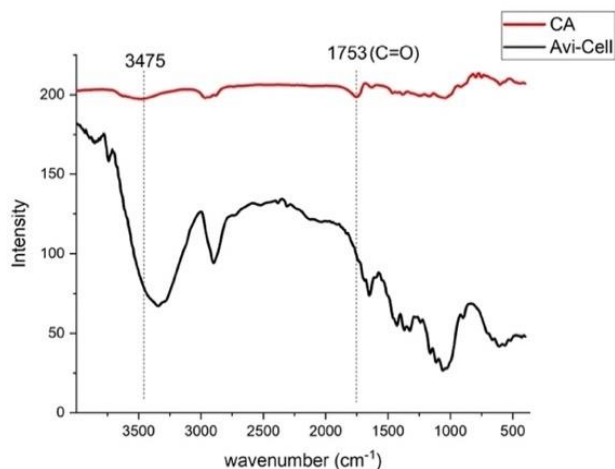


Figure 2. FTIR spectrum of cellulose and cellulose acetate

The appearance of the fingerprint area absorption peaked at 1735 cm^{-1} indicating the presence of a C=O group originating from the acetyl group as evidence of the formation of CA. In addition, a decrease in the intensity of the -OH group stretching absorption in the 3400 cm^{-1} area indicated that an acetyl group had replaced the OH group [23]. This was supported by a previous study by Liu [24], who synthesized CA from commercial cellulose and reported that the appearance of absorption in the 1730 cm^{-1} area indicated that CA was successfully synthesized.

3.2 CA/PEG membrane fabrication

CA-based membranes were successfully synthesized with various composition variations of CA as a polymer matrix, PEG as a stabilizer and pore former agent, and DMF as a solvent. Figure 3 visualized the membrane and the composition variations used were presented in detail in Table 1.

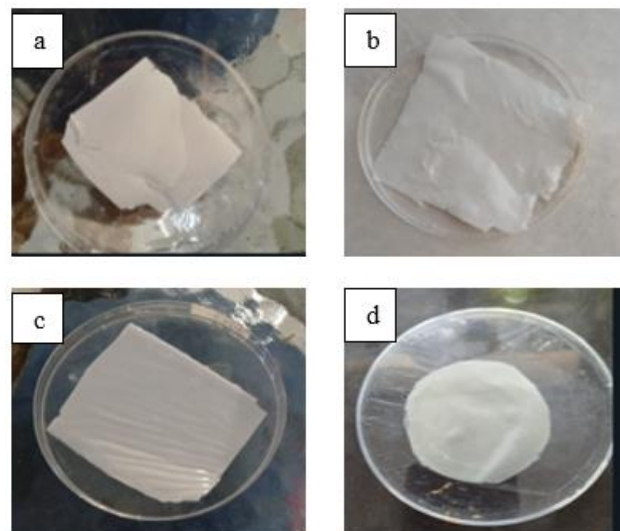


Figure 3. Cellulose acetate-based membrane (a) CA/PEG (15:3), (b) CA/PEG (14:4), (c) CA/PEG (13:5), (d) CA/PEG (12:6)

Figure 3 illustrated a white CA/PEG membrane with a thickness ranging from 0.1 to 0.2 mm. The membrane with a CA ratio of 15:3 exhibited the highest thickness, a rougher surface texture, and was prone to breakage. This could be attributed to the high CA polymer content, which was not sufficiently balanced by PEG, a component that served to stabilize the surface [25, 26]. From the results obtained, the best composition based on visualization and membrane elasticity was a ratio of 13:5. This formulation produced a membrane with minimal thickness while exhibiting enhanced elasticity. Moreover, these findings highlighted the crucial role of PEG as a stabilizer and plasticizer, underscoring the importance of achieving an appropriate balance in the composition.

Table 1. Variations in the composition of CA/PEG, thickness, and membrane visualization

CA (%)	PEG (%)	DMF (%)	Vol. of solution (mL)	Thickness (mm)	Membrane Condition
12	6	82	10	0.14	More elastic and transparent
13	5	82	10	0.17	More elastic and transparent
14	4	82	10	0.21	Less elastic, not transparent
15	3	82	10	0.24	Easy to break, rough surface, and not transparent

3.3 Physicochemical properties of the membrane

3.3.1 Water contact angle

Figure 4 shows a photo capture of the measurement of the water contact angle on the membrane using the ImageJ program.

Table 2. The water contact angle of the membrane CA/PEG

Type of Membrane	WCA
CA/PEG (12:6)	59.621°
CA/PEG (13:5)	64.587°
CA/PEG (14:4)	75.011°
CA/PEG (15:3)	75.467°

The water contact angle on various CA/PEG membranes was summarized in Table 2, where it could be seen that the CA/PEG (12:6) membrane had a much smaller contact angle

than the other membranes. This indicated that the membrane absorbed water more quickly because it had a higher wetting or water distribution pattern. Increasing the PEG content in cellulose acetate (CA)-based membranes significantly enhances the hydrophilic properties of the membrane by altering its structure and promoting intermolecular interactions. The ether group (-C-O-C-) in PEG facilitates the formation of hydrogen bonds with water molecules, thereby improving the membrane's water absorption capacity [27]. Moreover, a higher PEG concentration generates micro water channels within the membrane matrix, which enhance water molecule transport and lower flow resistance. Conversely, a reduced PEG content results in a denser membrane structure, which restricts water penetration and diminishes the overall hydrophilicity of the membrane. The hydrophilic nature of PEG made it easier for the CA/PEG (12:6) membrane to attract water [16]. These results followed the membrane swelling value, where the CA/PEG (12:6) membrane had the highest

swelling value, which correlated with the high hydrophilicity of the membrane. Figure 4 also showed that increasing the CA content and decreasing the PEG content caused an increase in the water contact angle, which indicated a decrease in the hydrophilicity of the membrane [26]. However, the water contact angle of all membranes was still below 90°, which meant that it was hydrophilic.

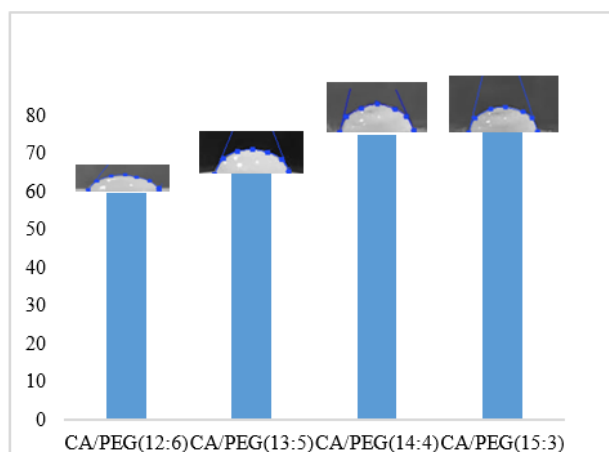


Figure 4. The water contact angle of each membrane CA/PEG

3.3.2 Swelling index

Table 3 indicated the results of the swelling test of the CA/PEG membrane, which showed that the most swelling was obtained in the CA/PEG membrane (12:6). The overall test results showed that the higher the CA content and the lower the PEG content, the lower the swelling. This was because CA was more hydrophobic (does not like water), and PEG was more hydrophilic, and when the CA was more, the diffusion of water through the membrane was lower [25].

Table 3. Swelling index of each CA/PEG membrane

Membrane	Initial Weight (g)	Final Weight (g)	Swelling Index (%)
CA/PEG (12:6)	0.16	0.29	81.25
CA/PEG (13:5)	0.14	0.23	64.28
CA/PEG (14:4)	0.22	0.31	40.91
CA/PEG (15:3)	0.27	0.38	40.74

3.4 FTIR analysis

Figure 5 shows the difference in FTIR spectra results of CA, PEG, and CA/PEG membranes at various composition ratios. As previously explained, in the cellulose acetate spectrum, there are absorption peaks at 3400 cm⁻¹ from the hydroxyl group and 1735 cm⁻¹ from the acetyl group of CA. After membrane formation, the absorption band width of the -OH group increases in intensity and shifts to the 3300-3100 cm⁻¹ region due to the penetration of the -OH group from PEG to the O atom which has a free electron in the acetyl group of CA. Likewise, the acetyl group shifts to the 1730 cm⁻¹ region due to some of the acetyl groups being substituted by the OH group from PEG, and its intensity increases with increasing PEG concentration (the reaction mechanism for the formation of the

CA/PEG membrane) can be seen in Figure 6). The successful formation of membranes from cellulose acetate (CA) and polyethylene glycol (PEG) was confirmed by the absorption peak associated with the presence of C-O vibrations in the 1049 cm⁻¹ region, which confirmed the formation of new bonds between CA and PEG [18]. This is supported by the research of Fathy et al. [12] which confirmed the formation of new C-O bonds after the fabrication of PES/CA/PEG membranes in the area around 1050-1100 cm⁻¹. In addition, a torsional O-H group peak also appeared in the 617-619 cm⁻¹ region throughout the membrane spectrum, although with low intensity. Furthermore, the characteristic peaks of CA were still observed in the membrane, including the bending vibration of the C-H group at 1320 cm⁻¹ [28, 29].

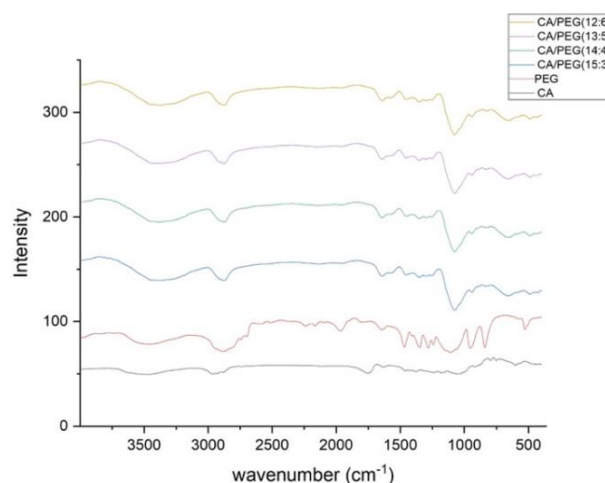


Figure 5. FTIR spectra of CA, PEG, and each CA/PEG membrane

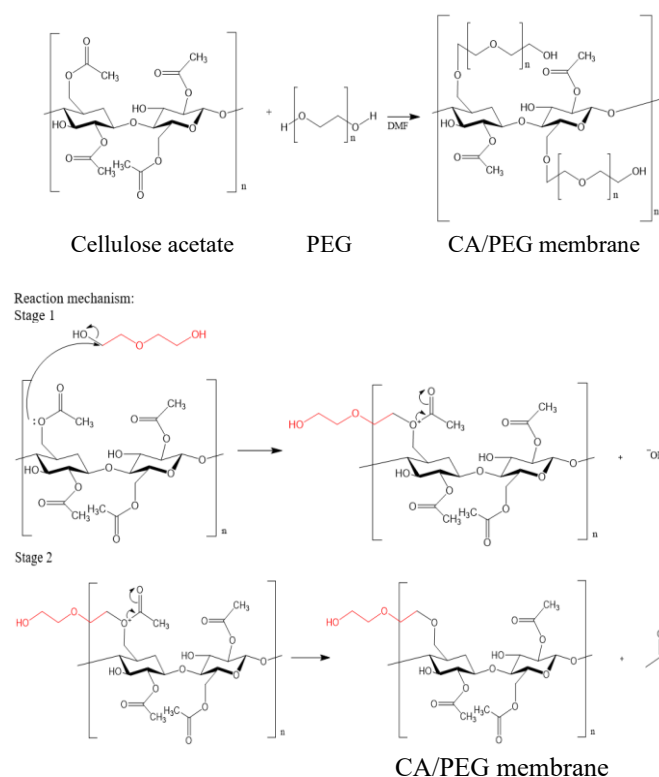


Figure 6. Reaction mechanism of CA/PEG membrane formation

3.5 SEM analysis

Figure 7 presents SEM analysis of the CA/PEG (14:4) membrane, revealing the top surface layer at 50x magnification with pores of diverse and irregular sizes. These were not well distributed and smooth, with some pores quite far apart, implying that the membrane surface was classified as slightly porous. The analysis showed that one of the pores was sized 20 μm , indicating that the membrane pores were still in the microporous category.

The ratio of CA and PEG composition, as well as the compatibility of solvents and pore-forming agents, were all critical factors in pore formation. The phase inversion procedure that changed the dope polymer from a liquid to a solid must be controlled with various parameters [30-32]. Controlling this was essential to maintaining selectivity during membrane fabrication. Therefore, it was essential to formulate the membrane with the right amount of pore-forming agent. In the cross-section of the membrane thickness, it could be seen that the membrane was 2-layered, with several fractures between the layers and on the top.

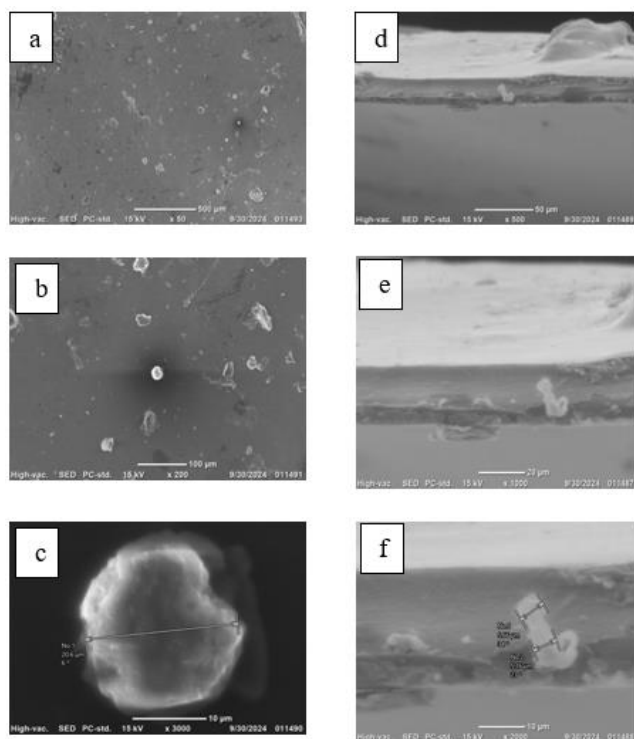


Figure 7. a) Morphology of surface CA/PEG (14:4) at 50x magnification, b) CA/PEG (14:4) at 200x magnification, c) morphology and analysis of pore diameter in CA/PE (14:4) at 3000x magnification, d) morphology of cross-section of CA/PEG (14:4) at 500x magnification, e) cross-section of CA/PEG (14:4) 1000x magnification, and f) fracture analysis in cross-section of CA/PEG (14:4) at 2000x magnification

3.6 TGA analysis

As illustrated in Figure 8, all membranes underwent three stages of thermal decomposition. The first stage, occurring between 40-90°C, corresponded to water evaporation, while the second stage, between 197-227°C, involved the degradation of the bonds between CA and PEG. At 241-300°C, the final stage was the decomposition of the remaining organic groups originating from CA compounds and the

degradation of cellulose and PEG chains. Based on the percentage of weight loss from the 3 membranes, the membrane with the composition of CA/PEG 14:4 had the lowest weight loss percentage at 70.64%, indicating that the membrane with this composition had the best thermal properties, while the CA/PEG membrane (12:6) and CA/PEG membrane (15:3) had a weight loss percentage of 73.52% and 71.48%, respectively.

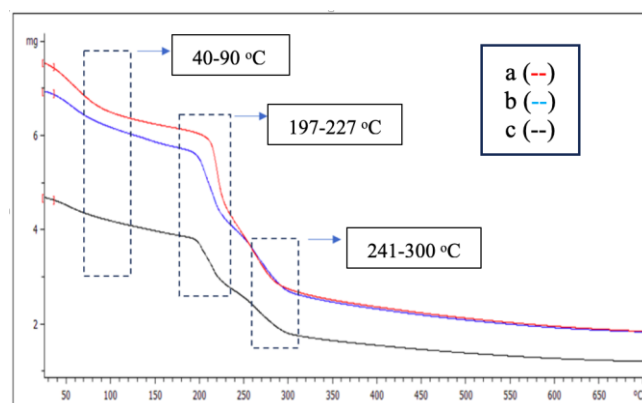


Figure 8. Thermograms of CA/PEG membranes (a) ratio 12:6, (b) 14:4, (c) 15:3 (wt)

The thermal stability of CA/PEG membranes is significantly influenced by the ratio of CA to PEG due to the chemical interactions between these components. Cellulose acetate exhibits strong intramolecular bonds and stable polymeric structure at elevated temperatures. On the other hand, the incorporation of PEG introduces ether groups (-C-O-C) that facilitate the formation of C-O bonds with the hydroxyl and acetyl groups of CA. This interaction enhances structural cohesion within the membrane, thereby mitigating thermal degradation [18]. However, an excessive PEG content can increase the amorphous nature of the membrane, diminishing its thermal stability. In the CA/PEG (12:6) membrane, the higher PEG content contributes to a more amorphous structure, reducing the density of intermolecular interactions and making the membrane more susceptible to thermal degradation. In contrast, the CA/PEG (15:3) membrane demonstrates better thermal stability due to a reduced PEG ratio, which maintains structural integrity. However, the lower PEG content limits the extent of C-O bond formation necessary for further enhancing thermal resistance [27].

3.7 Application of membrane in PAHs removal

3.7.1 Water flux

Table 4 indicates the results of membrane performance tests in the form of water flux. The results showed that the CA/PEG membrane had a reasonably high water flux value in the 43 - 54 L/m².hour with a feed volume of 100 mL for 7.5 minutes. This also showed that the membrane with the highest PEG content had the highest flux value of 54.081 L/m².hour. In addition, this aligns with the results of the swelling and water contact angle tests, where the membrane also had the highest value. This was because the hydrophilic nature of PEG made it easy for water to diffuse through the membrane [30].

Adding PEG to the more hydrophobic CA membrane matrix could increase the number of hydrophilic groups (-OH) on the membrane surface. These groups easily interact with water,

causing water to spread more evenly on the surface and reducing the water contact angle, ultimately increasing water flux. The higher the PEG content in the membrane matrix, the higher the water flux. Conversely, water flux decreased when the CA content was increased. This is undoubtedly due to the hydrophobic nature of CA, which had acetyl groups (-COOH) that made it more challenging to attract water [18, 26].

Table 4. Water flux of each CA/PEG membrane

Membrane	Surface Area (m ²)	Vol. Permeate (L)	Flux (L/m ² .h)
CA/PEG (12:6)	78.5×10 ⁻⁴	53×10 ⁻³	54.081
CA/PEG (13:5)	78.5×10 ⁻⁴	46×10 ⁻³	46.938
CA/PEG (14:4)	78.5×10 ⁻⁴	47×10 ⁻³	47.959
CA/PEG (15:3)	78.5×10 ⁻⁴	43×10 ⁻³	43.877

3.7.2 Antifouling properties

The antifouling properties of CA/PEG membranes at various composition ratio variations were indicated by the magnitude of the FRR value, as seen in Table 5.

Table 5. The FRR value of CA/PEG membrane

Membrane	J _{wo} (LMH)	J _{wc} (LMH)	FRR (%)
CA/PEG (12:6)	54.081	36.852	68.142
CA/PEG (13:5)	46.938	35.716	76.091
CA/PEG (14:4)	47.959	40.583	84.620
CA/PEG (15:3)	43.877	33.972	77.425

The results showed that the highest FRR value was obtained on the CA/PEG (14:4) membrane of 84.620%. This meant that the membrane had good antifouling properties. The higher the FRR value, the better the antifouling properties. Although it played a role in increasing water flux, as previously explained, the presence of PEG, which was hydrophilic in the membrane and acted as a stabilizing agent, could reduce the antifouling properties of the membrane [10]. The test results showed that the membrane with the highest PEG composition produced the lowest FRR percentage, which meant that its antifouling properties were lower. This was supported by Loske et al. [28], who modified the polysulfone RO membrane with the addition of PEG, which also resulted in a decrease in antifouling properties in high salinity conditions of the feed solution.

3.7.3 PAHs rejection

Table 6 indicated that Marine Sediment Extract (MSE) from the Makassar Strait contained 3 types of PAHs compounds including benzo(a)anthracene, pyrene, and perylene. The benzo(a)anthracene compound had the highest concentration of 2,162 ppm at TG₁ and TG₂, followed by perylene at 1,639 ppm at all stations and pyrene at 0.003 ppm at all stations. In addition, out of the 3 compounds detected, benzo(a)anthracene and perylene compounds were above the threshold of PAHs compounds in seawater [33], while the pyrene compound was still within safe limits [31].

Based on Table 7, the rejection of CA/PEG membranes against real MSE samples containing PAHs compounds (pyrene, benzo(a)anthracene, perylene) was shown. The results of the analysis showed that all types of CA/PEG membranes had very good rejection properties against PAHs compounds. Based on GC-MS analysis, of the 3 PAHs

compounds contained in the sediment extract, only pyrene was detected at a fairly low concentration after the filtration process with the CA/PEG membrane. Benzo(a)anthracene and perylene were not detected, indicating that both compounds were retained on the membrane. This was supported by the results of the FTIR analysis of the membrane after the filtration process, which showed different peaks from the membrane before filtration (see Figure 9). Typical peaks of the CA/PEG membrane such as the OH group in the 3300-3400 cm⁻¹ region, the C=O group of CA in the 2900 cm⁻¹ region, and the torsional OH group in the 600-617 cm⁻¹ region were significantly not observed and shifted after the membrane was treated in the filtration process.

Table 6. The concentration of PAHs in marine sediment extract from 3 stations in Makassar Strait, Indonesia

PAHs Standard	TG ₁ (ppm)	TG ₂ (ppm)	TG ₃ (ppm)
Naphthalene	-	-	-
Acenaphthene	-	-	-
Phenanthrene	-	-	-
Fluoranthene	-	-	-
Pyrene	0.003	0.003	0.003
Benzo(a)anthracene	2.162	2.162	2.161
Perylene	1.639	1.639	1.639

Table 7. The PAHs content in EMS after filtration

Membrane	EMS Content					
	Benzo(a)anthracene		Pyrene		Perylene	
	C _f	C _p	C _f	C _p	C _f	C _p
CA/PEG (12:6)	2.162	nd	0.003	0.0016	1.639	nd
CA/PEG (13:5)	2.162	nd	0.003	0.0024	1.639	nd
CA/PEG (14:4)	2.162	nd	0.003	0.0012	1.639	nd
CA/PEG (15:3)	2.162	nd	0.003	0.0027	1.639	nd

*nd (not detected), EMS (extract of marine sediment), C_f (PAHs concentration in EMS before filtration), C_p (PAHs concentration after filtration).

Table 8. The rejection of membrane to pyrene

Membrane	C _f (ppm)	C _p (ppm)	R (%)
CA/PEG (12:6)	0.003	0.0009	70.00
CA/PEG (13:5)	0.003	0.00054	82.00
CA/PEG (14:4)	0.003	0.00037	87.67
CA/PEG (15:3)	0.003	0.00038	87.33

Table 8 exhibited the rejection percentage of various CA/PEG membranes towards pyrene. This rejection value indicated the ability of the membrane to filter PAHs compounds during the filtration process. The higher the rejection percentage, the more effective the membrane was in preventing pyrene from passing through the membrane. The CA/PEG (12:6) membrane showed a lower rejection percentage of 70.00%, while the CA/PEG (13:5), (14:4), and (15:3) membranes showed much higher rejections of 82.00%, 87.67%, and 87.33%, respectively. The increase in the rejection percentage with changes in the CA: PEG ratio indicated that the membrane composition played an important role in its efficiency in rejecting PAHs compounds. Membranes with higher CA content had stronger hydrophobic interactions, which could increase the membrane's ability to reject hydrophobic compounds such as pyrene. This was because hydrophobic molecules tended to interact less with more hydrophilic membranes and were, therefore, more easily

retained [17, 21]. This also occurred in benzo(a)anthracene and perylene compounds which had stronger hydrophobic properties than pyrene [17].

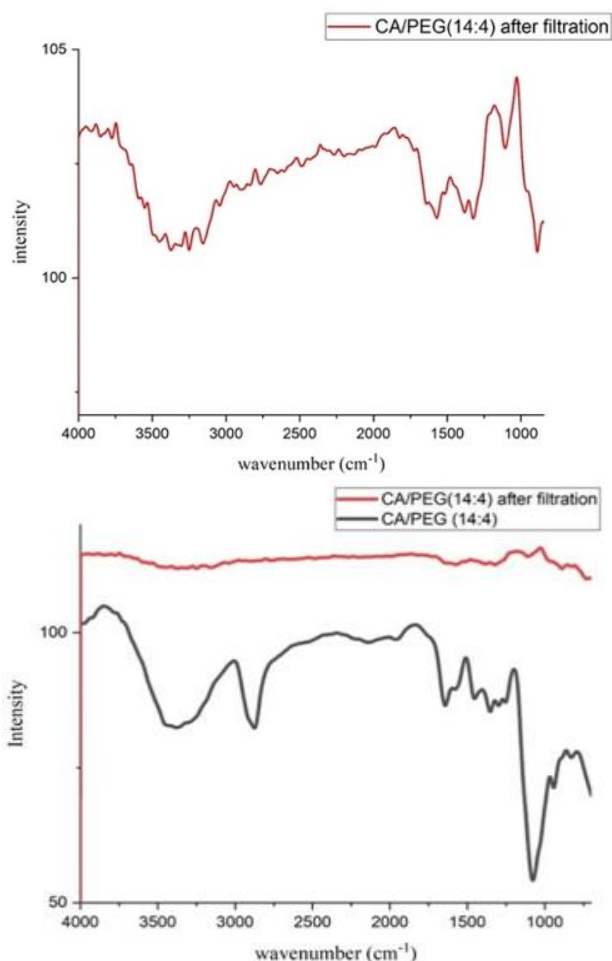


Figure 9. FTIR spectra of CA/PEG membrane 14:4 before and after filtration treatment

4. CONCLUSION

CA-based composite membranes were successfully synthesized by adding PEG as a stabilizer and pore-forming agent in various composition ratio variations. Based on the results of SEM analysis, the membranes showed less porous surface characteristics. The performance test results showed that the CA/PEG membrane had high efficiency in rejecting PAH, with the rejection percentage reaching 70-87% for pyrene compounds, while for benzo(a)anthracene and perylene compounds it reached 100%. In addition, the membrane with a CA/PEG ratio of 14:4 (w/w) had the best antifouling properties with an FRR value of 84.62% which showed the potential of the membrane to support a hydrodynamically efficient filtration process, thereby reducing the energy required during the separation process. On the other hand, the source of cellulose acetate as the main material in the formation of the membrane has a high abundance and environmentally friendly, so that the membrane can be used sustainably.

ACKNOWLEDGMENT

This work was supported by DRTPM Ministry of Education, Culture, Study, and Technology of Indonesia in the scheme of Fundamental Report Scheme Contract No.: 2864/UN36.11/LP2M/2024 and Lembaga Penelitian dan Pengabdian Masyarakat (LP2M) Universitas Negeri Makassar that had held writing workshops of scientific articles in reputable international journals as a forum for the creation of this study article.

REFERENCES

- [1] Wang, J., Wang, G., Zhang, Z., Hao, J. (2024). Characteristics of polycyclic aromatic hydrocarbons (PAHs) removal by nanofiltration with and without coexisting organics. *Chemosphere*, 295(4): 141426. <https://doi.org/10.1016/j.chemosphere.2024.141426>
- [2] Chen, X., Huang, G., An, C., Feng, R., Wu, Y., Huang, C. (2022). Superwetting polyethersulfone membrane functionalized with ZrO₂ nanoparticles for polycyclic aromatic hydrocarbon removal. *Journal of Material Science Technology*, 98(3): 14-25. <https://doi.org/10.1016/j.jmst.2021.01.063>
- [3] Syahrir, M., Yulianti, Wijaya, M., Zulfikar, Magfirah, N. (2021). The Characteristics of Naphthalene and Phenanthrene as Polycyclic Aromatic Hydrocarbons (PAHs) Compounds in the Marine Sediment of Tanjung Bayang Beach in Makassar. *Journal of Physics: Conference Series*, 1899(1): 012033. <https://doi.org/10.1088/1742-6596/1899/1/012033>
- [4] Costa, J.A.S., Sarmiento, V.H.V., Romão, L.P.C., Paranhos, C.M. (2020). Removal of polycyclic aromatic hydrocarbons from aqueous media with polysulfone/MCM-41 mixed matrix membranes. *Journal of Membrane Science*, 601(1): 117912. <https://doi.org/10.1016/J.MEMSCI.2020.117912>
- [5] Amorini, M. (2022). Reusable Cavitand-Based Electrospun Membranes for the Removal of Polycyclic Aromatic Hydrocarbons from Water. *Small*, 18(1): 433-440. <https://doi.org/10.1002/SMLL.202104946>
- [6] Zango, Z.U. (2020). An overview and evaluation of highly porous adsorbent materials for polycyclic aromatic hydrocarbons and phenols removal from wastewater. *Water (Switzerland)*, 12(10): 1-40. <https://doi.org/10.3390/W12102921>
- [7] Xu, J., Zhu, C., Song, S., Fang, Q., Zhao, J., Shen, Y. (2021). A nanocubicle-like 3D adsorbent fabricated by in situ growth of 2D heterostructures for removal of aromatic contaminants in water. *Journal of Hazard Materials*, 423: 127004. <https://doi.org/10.1016/J.JHAZMAT.2021.127004>
- [8] Dai, Y., Niu, J., Yin, L., Xu, J. (2013). Laccase-carrying electrospun fibrous membrane for the removal of polycyclic aromatic hydrocarbons from contaminated water. *Purify Technology*, 104(2): 1-8. <https://doi.org/10.1016/J.SEPPUR.2012.11.013>
- [9] Ahmad, A. (2016). Self-sterilized composite membranes of cellulose acetate/polyethylene glycol for water desalination. *Carbohydrate Polymers*, 149: 207-216. <https://doi.org/10.1016/J.CARBPOL.2016.04.104>
- [10] Chen, G.Q., Kanehashi, S., Doherty, C.M., Hill, A.J., Kentish, S.E. (2015). Water vapor permeation through cellulose acetate membranes and its impact upon membrane separation performance for natural gas

- purification. *Journal of Membrane Science*, 487(3): 249-255. <https://doi.org/10.1016/J.MEMSCI.2015.03.074>
- [11] Abedini, R., Mousavi, S.M., Aminzadeh, R. (2011). A novel cellulose acetate (CA) membrane using TiO₂ nanoparticles: Preparation, characterization and permeation study. *Desalination*, 277(1-3): 40-45. <https://doi.org/10.1016/J.DESAL.2011.03.089>
- [12] Fathy, M., Ali, H.R., Moustafa, Y.M., El Shahawy, A. (2020). Removal of suspended matter and salts on ultrafiltration cellulose acetate/expanded polystyrene waste grafted PEG composite membrane. *Desalination and Water Treatment*, 197: 30-40. <https://doi.org/10.5004/DWT.2020.25960>
- [13] Bhattacharjee, C., Datta, S. (2003). Analysis of polarized layer resistance during ultrafiltration of PEG-6000: An approach based on filtration theory. *Purify Technology*, 33(2): 115-126. [https://doi.org/10.1016/S1383-5866\(02\)00142-9](https://doi.org/10.1016/S1383-5866(02)00142-9)
- [14] Vatanpour, V. (2022). Cellulose acetate in fabrication of polymeric membranes: A review. *Chemosphere*, 295(4): 133914. <https://doi.org/10.1016/J.CHEMOSPHERE.2022.133914>
- [15] Ahmad, A. (2015). Effect of silica on the properties of cellulose acetate/polyethylene glycol membranes for reverse osmosis. *Desalination*, 355: 1-10. <https://doi.org/10.1016/J.DESAL.2014.10.004>
- [16] Guo, H. (2020). Development and investigation of novel antifouling cellulose acetate ultrafiltration membrane based on dopamine modification. *International Journal of Biological Macromolecules*, 160: 652-659. <https://doi.org/10.1016/J.IJBIOMAC.2020.05.223>
- [17] Kim, H.Y., Cho, Y., Kang, S.W. (2019). Porous cellulose acetate membranes prepared by water pressure-assisted process for water-treatment. *Journal of Industrial and Engineering Chemistry*, 78(3): 421-424. <https://doi.org/10.1016/J.JIEC.2019.05.027>
- [18] Costa, R.E., Lobo-Recio, M.A., Battistelli, A.A., Bassin, J.P., Belli, T.J., Lapolli, F.R. (2018). Comparative study on treatment performance, membrane fouling, and microbial community profile between conventional and hybrid sequencing batch membrane bioreactors for municipal wastewater treatment. *Environmental Science and Pollution Research*, 25(32): 32767-32782. <https://doi.org/10.1007/S11356-018-3248-8>
- [19] Sun, Z. (2025). Enhancement of antifouling and separation properties of poly(m-phenylene isophthalamide) hybrid ultrafiltration membrane using highly crystalline poly(heptazine imide) nanosheets. *Journal of Membrane Science*, 713(1): 123340. <https://doi.org/10.1016/J.MEMSCI.2024.123340>
- [20] Syahrir, M. (2018). The content of Polycyclic Aromatic Hydrocarbons (PAH) in the green mussels (*Perna Viridis*) around the coast of Makassar. In *Journal of Physics: Conference Series*, IOP Publishing, 1028(1): 012037. <https://doi.org/10.1088/1742-6596/1028/1/012037>
- [21] Abdelhamid, A.E., Khalil, A.M. (2019). Polymeric membranes based on cellulose acetate loaded with candle soot nanoparticles for water desalination. *Journal of Macromolecular Science, Part A: Pure and Applied Chemistry*, 56(2): 153-161. <https://doi.org/10.1080/10601325.2018.1559698>
- [22] Rana, J., Goindi, G., Kaur, N., Krishna, S., Kakati, A. (2022). Synthesis and application of cellulose acetate-acrylic acid-acrylamide composite for removal of toxic methylene blue dye from aqueous solution. *Journal of Water Process Engineering*, 49: 103102. <https://doi.org/10.1016/J.JWPE.2022.103102>
- [23] Hu, Z., Zhang, H., Zhang, X.F., Jia, M., Yao, J. (2022). Polyethylenimine grafted ZIF-8@cellulose acetate membrane for enhanced gas separation. *Journal of Membrane Science*, 662: 120996. <https://doi.org/10.1016/J.MEMSCI.2022.120996>
- [24] Liu, B. (2016). Thin-film composite forward osmosis membranes with substrate layer composed of polysulfone blended with PEG or polysulfone grafted PEG methyl ether methacrylate. *Frontiers of Chemical Science and Engineering*, 10(4): 562-574. <https://doi.org/10.1007/s11705-016-1588-9>
- [25] Liang, S., Zou, J., Meng, L., Fu, K., Li, X., Wang, Z. (2024). Impacts of high salinity on antifouling performance of hydrophilic polymer-modified reverse osmosis (RO) membrane. *Journal of Membrane Science*, 708: 123042. <https://doi.org/10.1016/J.MEMSCI.2024.123042>
- [26] Rana, J., Goindi, G., Kaur, N., Sahu, O. (2022). Optimization and synthesis of cellulose acetate based grafted gel and study of swelling characteristics. *Materials Today: Proceedings*, 48(4): 1614-1619. <https://doi.org/10.1016/J.MATPR.2021.09.500>
- [27] Wang, C. (2012). Click poly(ethylene glycol) multilayers on RO membranes: Fouling reduction and membrane characterization. *Journal of Membrane Science*, 409-410: 9-15. <https://doi.org/10.1016/j.memsci.2012.02.049>
- [28] Loske, L., Nakagawa, K., Yoshioka, T., Matsuyama, H. (2020). 2D nanocomposite membranes: Water purification and fouling mitigation. *Polymers*, 231(4): 127-135. <https://doi.org/10.3390/membranes10100295>
- [29] Junker, M.A., te Brinke, T., Vall Compte, C.M., Lammertink, R.G.H., de Grooth, J., de Vos, W.M. (2023). Asymmetric polyelectrolyte multilayer nanofiltration membranes: Structural characterisation via transport phenomena. *Journal of Membrane Science*, 681: 121718. <https://doi.org/10.1016/j.memsci.2023.121718>
- [30] Fernández-Sempere, F., Ruiz-Beviá, R., Salcedo-Díaz, P., García-Algado, García-Rodríguez, M. (2012). Digital holographic interferometry visualization of PEG-10000 accumulation on an acetate cellulose membrane: assessment of polarization layer and adsorption phenomenon. *Desalination and Water Treatment*, 42(1-3): 49-56. <https://doi.org/10.5004/DWT.2012.2454>
- [31] Syahrir, M., Nurul, H., Aprilita, Nuryono, Herawati, N. (2016). PAHs characteristics in sediment around Makassar coast using Gc-Fid. In *Makassar International Conference Sport and Medical Science MICSAMS, Makassar, Indonesia*.
- [32] Soursou, V., Campo, J., Picó, Y. (2023). Revisiting the analytical determination of PAHs in environmental samples: An update on recent advances. *Trends in Environmental Analytical Chemistry*, 37: e00195. <https://doi.org/10.1016/j.teac.2023.e00195>
- [33] Shami, R., Sabir, A., Iqbal, S.S., Gull, N., Zohra, R., Khan, S.M. (2023). Synergistic effect of GO/ZnO loading on the performance of cellulose acetate/chitosan blended reverse osmosis membranes for NOM rejection. *Heliyon*, 9(3): e13736. <https://doi.org/10.1016/J.HELİYON.2023.E13736>